

Supplementary Information for Does population structure predict the rate of speciation? A comparative test across Australia's most diverse vertebrate radiation

Sonal Singhal^{1,2}, Huateng Huang³, Maggie Grundler¹, María R. Marchán-Rivadeneira⁴,
Iris Holmes¹, Pascal O. Title¹, Stephen C. Donnellan^{5,6}, and Daniel L. Rabosky¹

¹Museum of Zoology and Department of Ecology and Evolutionary Biology, University
of Michigan, Ann Arbor, MI 48109

²Department of Biology, CSU Dominguez Hills, Carson, CA 90747

³College of Life Sciences, Shaanxi Normal University, Xi'an, China 710119

⁴Genomic Diversity Laboratory and Department of Ecology and Evolutionary Biology,
University of Michigan, Ann Arbor, MI 48109

⁵South Australian Museum, North Terrace, Adelaide 5000, Australia

⁶Australian Centre for Evolutionary Biology and Biodiversity, University of Adelaide,
Adelaide 5005, Australia

1 Tables

Table S1: Details on the individuals for which we generated ddRAD data, including their museum voucher id, latitude, longitude, nominal species, and raw number of sequencing pairs generated. Table included in DataDryad package, doi: 10.5061/dryad.j6823nt.

GenBank Accession	Species	locus	sample name
AF530196.1	<i>Eulamprus sokosoma</i>	16s	Esok2
AF530233.1	<i>Eulamprus sokosoma</i>	ND4	Esok2
AY308341.1	<i>Eremiascincus fasciolatus</i>	12s	E69
AY308192.1	<i>Eremiascincus fasciolatus</i>	16s	E69
GU046485.1	<i>Eulamprus leuraensis</i>	ND4	H26
HM852455.1	<i>Hemiergis decresiensis</i>	12s	HEMDESNSW1_NSW1
KU309146.1	<i>Lerista allanae</i>	12s	Leal2
KU309188.1	<i>Lerista allanae</i>	16s	Leal2
KU309230.1	<i>Lerista allanae</i>	ATP	Leal2
KU309273.1	<i>Lerista allanae</i>	ND4	Leal2
KU309167.1	<i>Lerista colliveri</i>	12s	Leco1
KU309209.1	<i>Lerista colliveri</i>	16s	Leco1
KU309251.1	<i>Lerista colliveri</i>	ATP	Leco1
KU309294.1	<i>Lerista colliveri</i>	ND4	Leco1
KU309299.1	<i>Lerista rochfordensis</i>	ND4	Lero2
KU309257.1	<i>Lerista rochfordensis</i>	ATP	Lero2
KU309215.1	<i>Lerista rochfordensis</i>	16s	Lero2
KU309173.1	<i>Lerista rochfordensis</i>	12s	Lero2
KU309174.1	<i>Lerista storri</i>	12s	LestA1
KU309216.1	<i>Lerista storri</i>	16s	LestA1
KU309258.1	<i>Lerista storri</i>	ATP	LestA1
KU309300.1	<i>Lerista storri</i>	ND4	LestA1
KU309306.1	<i>Lerista vittata</i>	ND4	LeviMC4
KU309267.1	<i>Lerista vittata</i>	ATP	LeviMC4
KU309224.1	<i>Lerista vittata</i>	16s	LeviMC4
KU309182.1	<i>Lerista vittata</i>	12s	LeviMC4
KJ505497.1	<i>Ctenotus kurnbudj</i>	cytb	NTMR20347

Table S2: Accession numbers for previously-published GenBank sequences used in phylogenetic inference.

analysis	short description	# of tips	phylogenetic signal	p-value	β_{IBD} and π	significance	β_{IBD} and limb reduction?	significance	β_{IBD} and speciation rate?	significance
a	bootstrap loci to calculate F_{ST}	104	0.34	0.01	1	0	1	0	0	0.48
b	bootstrap individuals to calculate F_{ST}	104	0.29	0.02	1	0.01	1	0	0	0.38
c	remove geographically-close F_{ST} comparisons	77	1.08	0.12	TRUE	0	TRUE	0	FALSE	0.65
d	remove extreme F_{ST} comparisons	77	0.39	0	TRUE	0.01	TRUE	0	FALSE	0.44
e	only desert	50	0.68	0.1	TRUE	0.03	TRUE	0.01	FALSE	0.56
f	remove <5 inds	77	0.38	0	TRUE	0	TRUE	0	FALSE	0.42
g	keep only significant IBD slopes	71	0.31	0.01	TRUE	0	TRUE	0	FALSE	0.18
h	drop young species	100	0.38	0.01	TRUE	0	TRUE	0	FALSE	0.65
i	random 80% of taxa	83	0.38	0.03	0.97	0.01	0.96	0.01	0.02	0.49
j	tree posterior	104	0.35	0.01	1	0	1	0	0.04	0.4
k	dxy slope across geography	105	0.00E+00	1	FALSE	0.39	TRUE	0	FALSE	0.94
l	fst slope across environmental distance	105	0.00E+00	1	TRUE	0	TRUE	0	FALSE	0.28

Table S3: Results from the series of analyses done to test the robustness of the results. Each analysis either recalculated extent of population structure (β_{IBD}) using different filters or included different taxonomic subsets based on filters. Analyses are lettered following their definition in text. Shown are the number of tips resulting after the filter was applied, the phylogenetic signal (λ) and its significance for β_{IBD} , if the relationship between within-population genetic diversity and β_{IBD} was significant, if the relationship between limb reduction and β_{IBD} was significant, and if the relationship between speciation rate (as estimated by λ_{DR}) and β_{IBD} was significant. For those analyses that were done across multiple iterations, values either reflect the mean value or the proportion of tests that were significant.

2 Figures

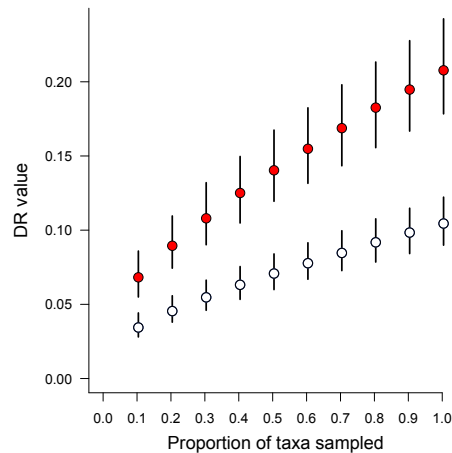


Figure S1: Distributions of λ_{DR} for constant-rate phylogenies as a function of taxon sampling. 2000 phylogenies of 100 taxa were simulated under fast ($\lambda = 0.15$, $\mu = 0$; solid red circles) and slow ($\lambda = 0.075$, $\mu = 0$; open circles) diversification processes; mean λ_{DR} was computed across all sampled tips for each tree. Points denote the median λ_{DR} value across 2000 trees for a given level of sampling; lines denote the 0.10 and 0.90 quantiles on the distribution of estimates. In this example, for two clades differing by a two-fold difference in the rate of speciation, only extreme differences in sampling could result in overlapping λ_{DR} distributions. For example, we would need to observe complete taxon sampling for the slow-rate clade and $\approx 20\%$ taxon sampling in the fast rate clade before these distributions showed appreciable overlap. Importantly, the variance in the distribution of λ_{DR} is relatively invariant with respect to the level of taxon sampling.

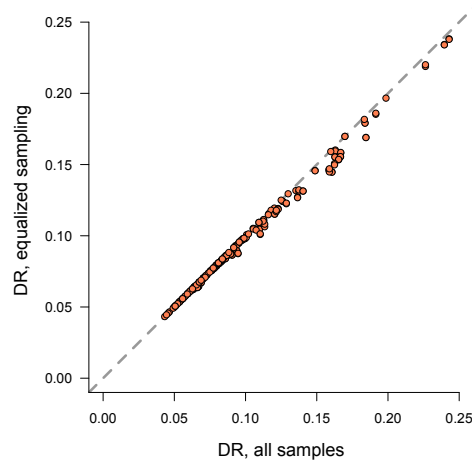


Figure S2: Rarefaction analysis to explore effects of among-clade variation in taxon sampling on λ_{DR} estimates. The phylogeny based on existing taxonomy contained 229 of 266 species, but taxon sampling varied among *Ctenotus* (93% of nominal species sampled), *Lerista* (83%), and other sphenomorphine lineages (80%). We simulated 500 taxon sets where we rarefied *Ctenotus* and *Lerista* sampling to equal that of the least-well sampled group (80%); thus, each subsampled phylogeny contained 213 / 266 species. Plot shows pairwise relationships between species-mean λ_{DR} values from subsampled datasets and the corresponding values from the full tree (each point is a single species). There is a slight bias in λ_{DR} driven by proportionately higher *Ctenotus* sampling, but the effect is weak overall. Mean λ_{DR} values were only marginally affected by this sampling exercise for *Ctenotus* (93% sampling: $\lambda_{DR} = 0.107$; 80% sampling: $\lambda_{DR} = 0.103$) and even less so for *Lerista* (83% sampling: $\lambda_{DR} = 0.112$; 80% sampling: $\lambda_{DR} = 0.110$).

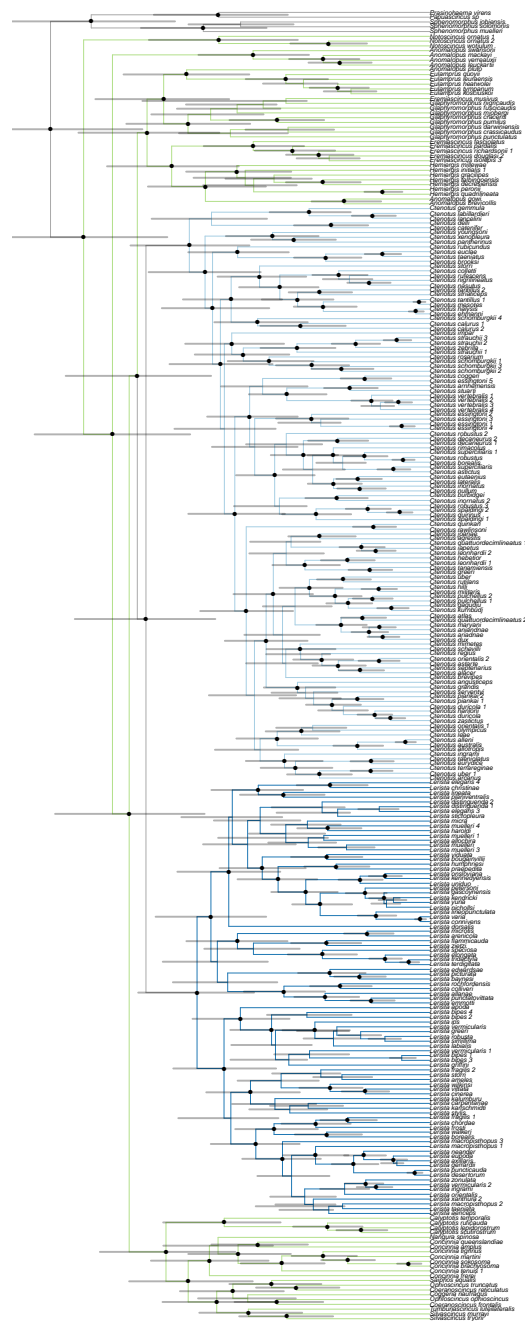


Figure S3: Phylogeny of sphenomorphine lizards used in this study, annotated to show posterior support for nodes and uncertainty in node height estimates. Clades are colored by genera: *Ctenotus* is shown in dark blue, *Lerista* in light blue, all other sphenomorphine genera in green, and the five outgroups in gray. Black circles at nodes mark nodes with $\geq 95\%$ posterior support. Gray bars at nodes indicate 95% highest posterior density for node height.

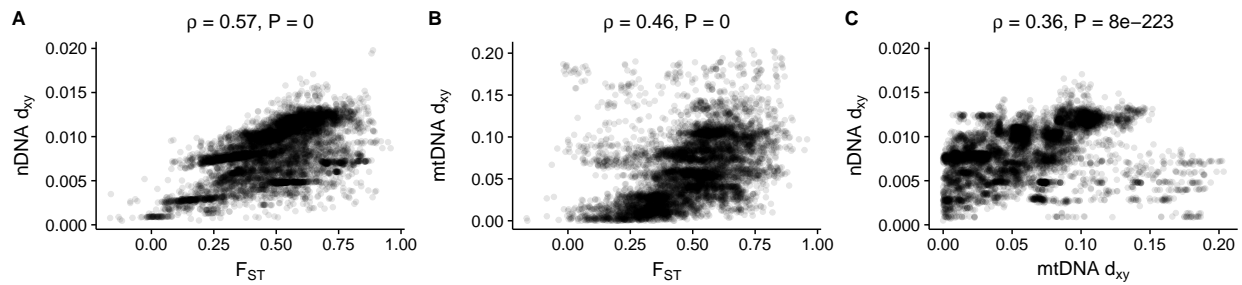


Figure S4: Correlations between measures of genetic distance inferred using three different metrics of pairwise genetic distance: D_{xy} based on nuclear data, D_{xy} based on mtDNA data, and F_{ST} based on nuclear data. Each point represents values estimated for a single individual. All correlations are significant, though correlations with mtDNA D_{xy} are weaker.

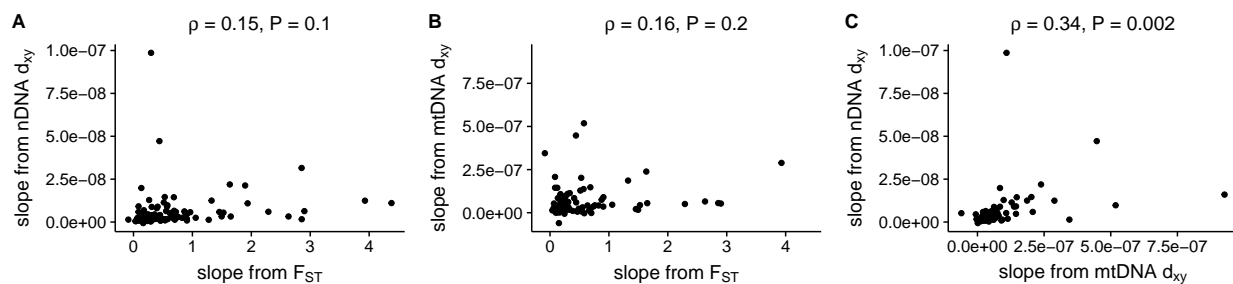


Figure S5: Correlations between isolation-by-distance patterns inferred using three different metrics of genetic distance: D_{xy} based on nuclear data, D_{xy} based on mtDNA data, and F_{ST} based on nuclear data (β_{IBD}). Each point represents values estimated for a single OTU. Only our two estimates based on D_{xy} values are significantly correlated.

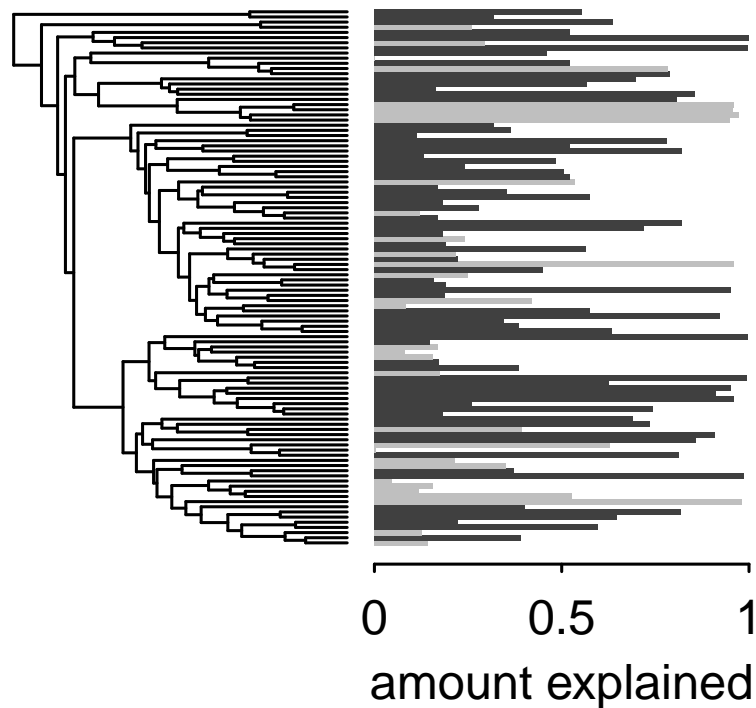


Figure S6: Phylogeny depicting the 104 operational taxonomic units (OTUs) included in this study and the proportion of the variance in F_{ST} values across the OTU that could be explained by an isolation-by-distance (IBD) model, as summarized by the correlation coefficient of a Mantel test of F_{ST} values against a geographic distances. A simple model of isolation-by-distance explained a substantial proportion of the variation in F_{ST} patterns across species (average $r^2 = 0.49$). Significant IBD relationships shown in black.

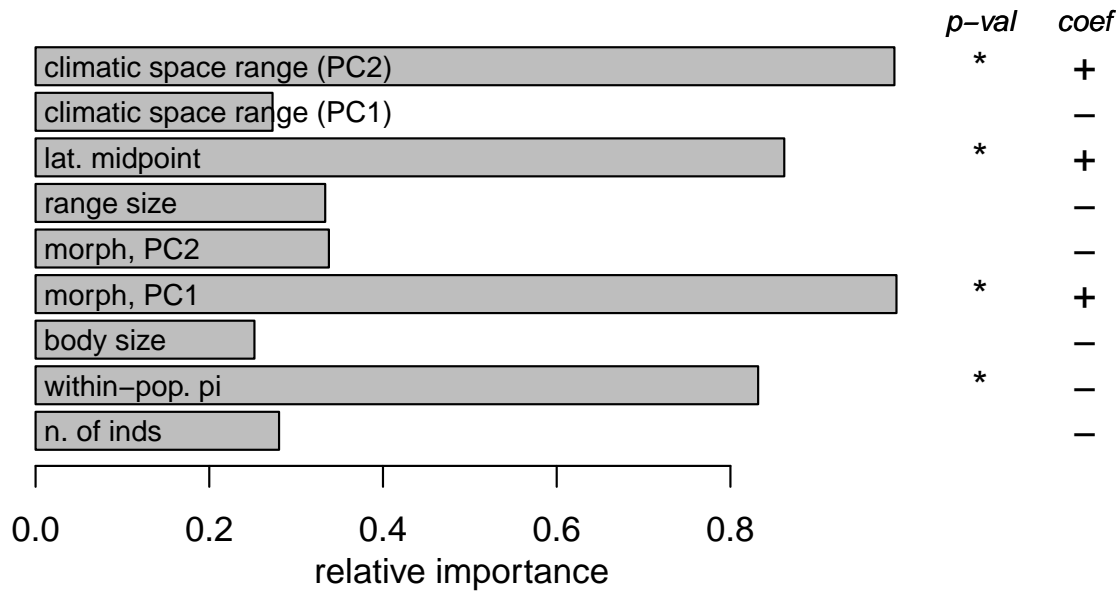


Figure S7: The results of our model-averaging approach testing three hypotheses for why extent of population structure (β_{IBD}) varies across species. To test if β_{IBD} varies as a function of deme size, we included the variables range size, body size, and within-population π . To test if β_{IBD} varies as a function of dispersal patterns, we included the variable morph, PC1, which reflects the degree of limb reduction and the variable morph, PC2, which reflects the degree of digit reduction. To test if β_{IBD} varies as a function of environmental heterogeneity, we included the range of climatic space exhibited by the species as summarized by two axes (PC1 and PC2). Finally, we included as nuisance variables the number of individuals sampled and the latitudinal midpoint of each species range. These results found significant support for within-population π , morphology PC1, range of climatic space (PC1), and latitudinal midpoint. However, climatic space (PC1) and latitudinal midpoint covary with biome (Fig. S8).

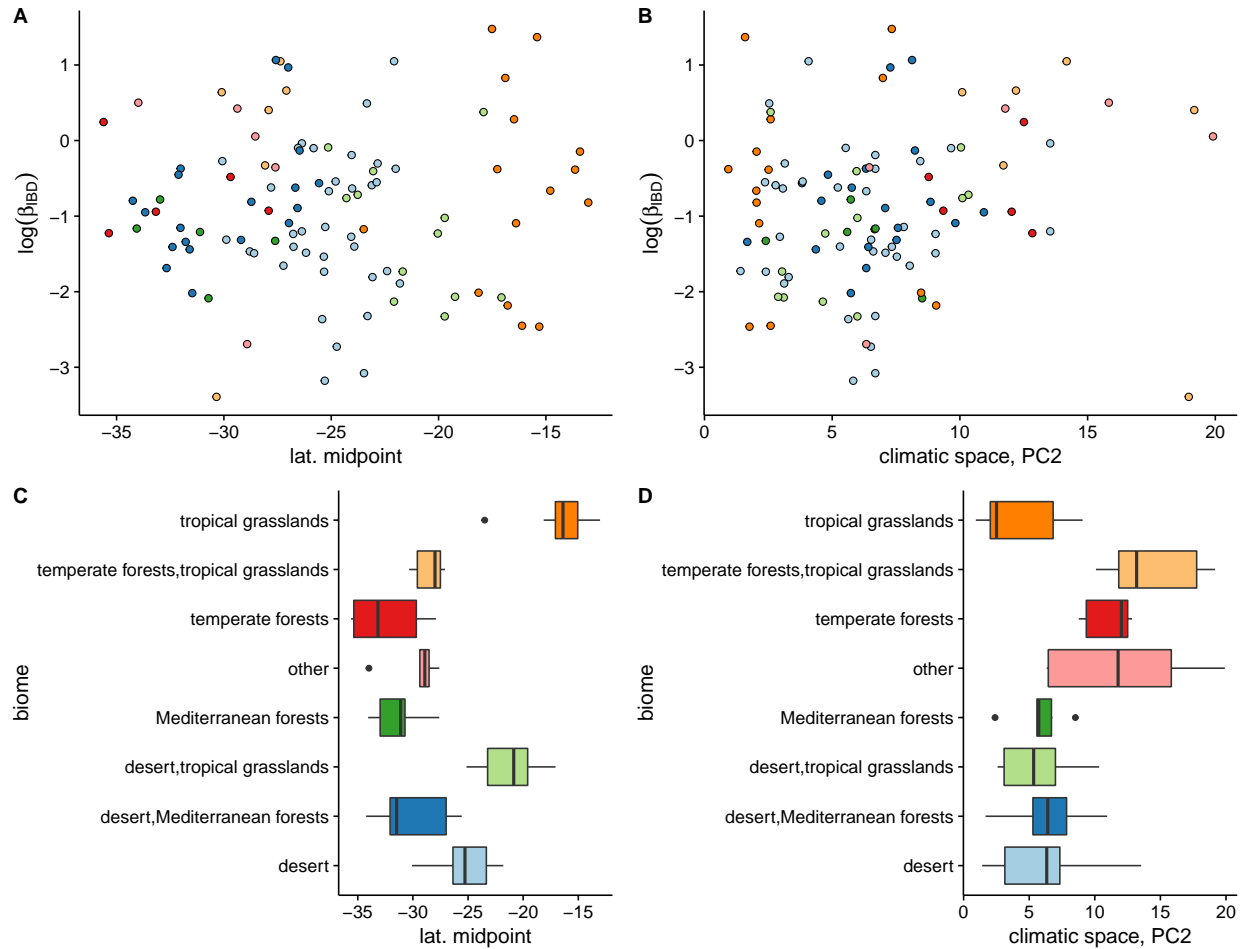


Figure S8: Correlation of significant spatial variables (A) latitudinal midpoint and (B) climatic space, PC2 with population structure (β_{IBD}). Points are colored by the biome in which each taxa occurs. Neither of these relationships is significant in single regression models, although they are significant predictors in our multiple regression model (Fig. S7). Latitudinal midpoint (C) and climatic space, PC2 (D) distributions across biomes. These two variables differ across biomes. In particular, high values for climatic space only occur in the tropical grasslands and temperate forest biomes in eastern Australia. Latitudinal midpoint and climatic space are not significant predictors of IBD if we restrict our analyses to those individuals found in the desert. This suggests these patterns are biome-specific. Because biomes can also vary in their biogeographic history, we refrain from discussing these results until additional data can verify these relationships are independent of biome.

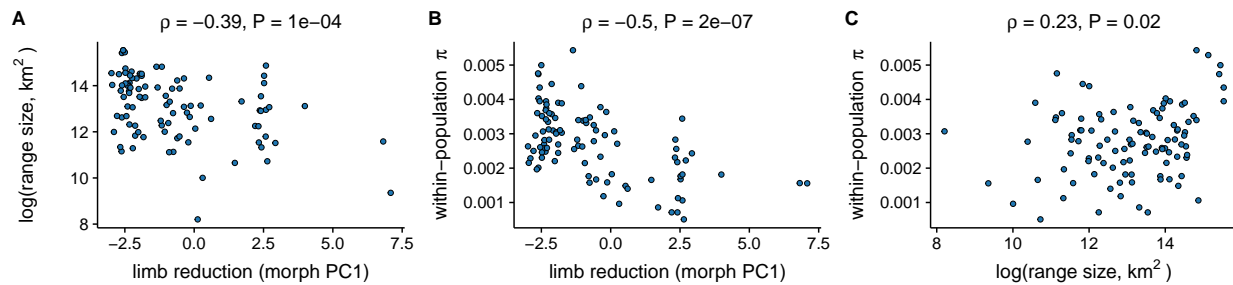


Figure S9: Correlations among range size, within-population π , and degree of limb reduction (morphology PC1) across the taxa included in this study. Two of the factors that predict extent of population structure (β_{IBD}) - within-population genetic diversity and degree of limb reduction - covary with each other and with range size. In general, species with reduced limbs tend to have smaller ranges and less genetic diversity.

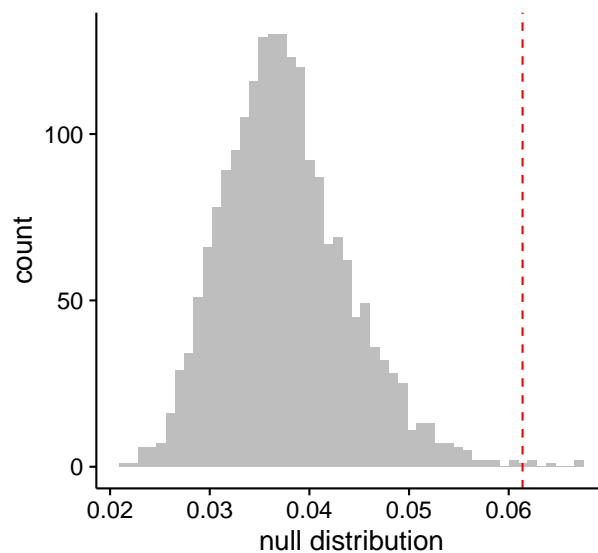


Figure S10: The distribution of tree imbalance extent (Colless's I_c) inferred across 2000 birth-death trees simulated with the same number of tips as the sphenomorphine tree. The red dotted-line indicates Colless's I_c for the true tree. The observed tree imbalance is significantly greater than expected under a random birth-death process (two-tailed p-value=0.005), which suggests there is heterogeneity in diversification rate across the sphenomorphine clade.

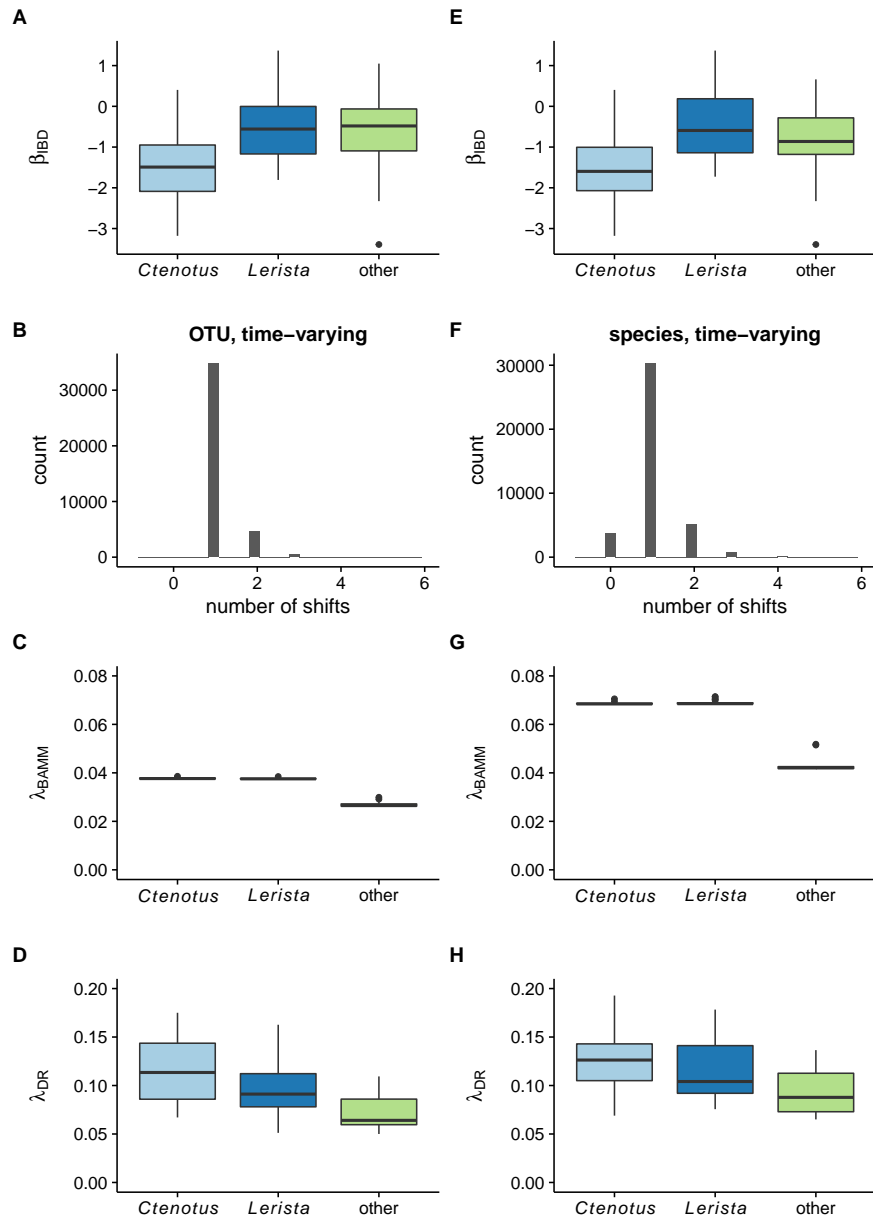


Figure S11: Differences in estimates of population structure (β_{IBD}) and speciation rates between two taxonomies: (A - D) operational taxonomic units (OTUs) as defined by GMYC and (E - H) nominal species as defined by the existing taxonomy. A and E depict β_{IBD} estimates. B and F depict the posterior distribution for number of speciation rate shifts detected by a time-varying model in BAMM. Under both phylogenies, the posterior distributions strongly supported one rate shift at the base of the *Ctenotus* and *Lerista* clade (Fig. 5). C and G show speciation rates as estimated by BAMM, and D and H show speciation rates as estimated by λ_{DR} . Estimates of speciation (λ_{BAMM}) are higher for the existing vs. revised taxonomy because (1) the two trees have slightly different root ages (30.6 Ma in OTU vs. 24.2 Ma in nominal species) and (2) the OTU tree shows greater evidence of slowdown as measured by γ . That said, the relative rates among groups are the same across both topologies, and absolute speciation rates as estimated by λ_{DR} are relatively and absolutely similar across groups. Thus, which taxonomy is used has no major qualitative impact on relative estimates of population structure or speciation rates.

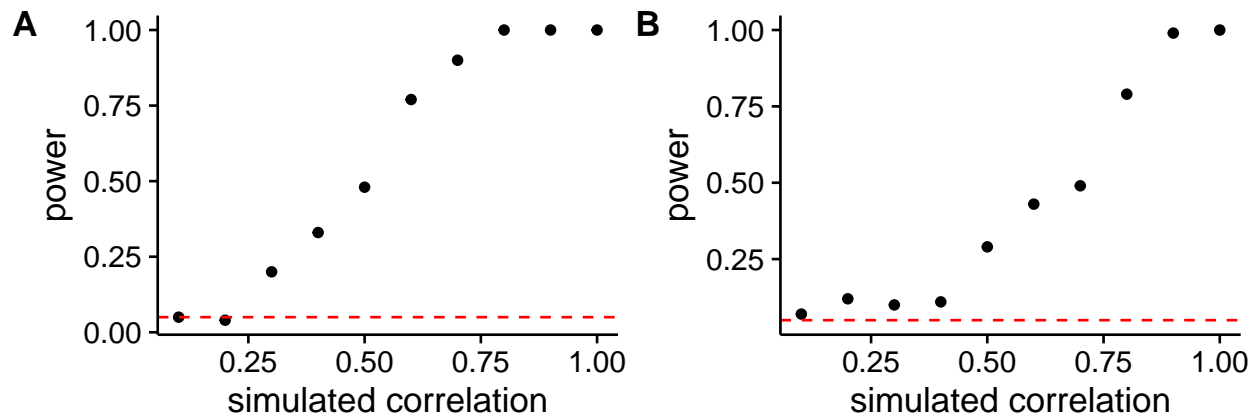


Figure S12: Power to detect a relationship between our trait of interest (β_{IBD}) and speciation rate as measured by the equal-splits measure λ_{DR} . We simulated trait values using a Brownian motion model on the phylogeny and rotated them with respect to speciation rates using true correlations (ρ) ranging from 0.1 to 1.0 in steps of 0.1. We then used the simulated values to test if there was a significant correlation between the trait values and speciation rates using (A) phylogenetic least squares (PGLS) and (B) ES-Sim. ES-Sim is a non-parametric approach that tests if an observed correlation between trait values and speciation rates is significantly different from correlations generated under a null model. Shown are the percentage of tests in which we recovered a significant correlation. The red dotted line indicates the percentage of tests for which we recovered a significant correlation when the data were uncorrelated ($\rho = 0$). We have limited power to detect a correlation unless it is substantial ($\rho \geq 0.6$), and, for this topology, PGLS has greater power than ES-Sim.

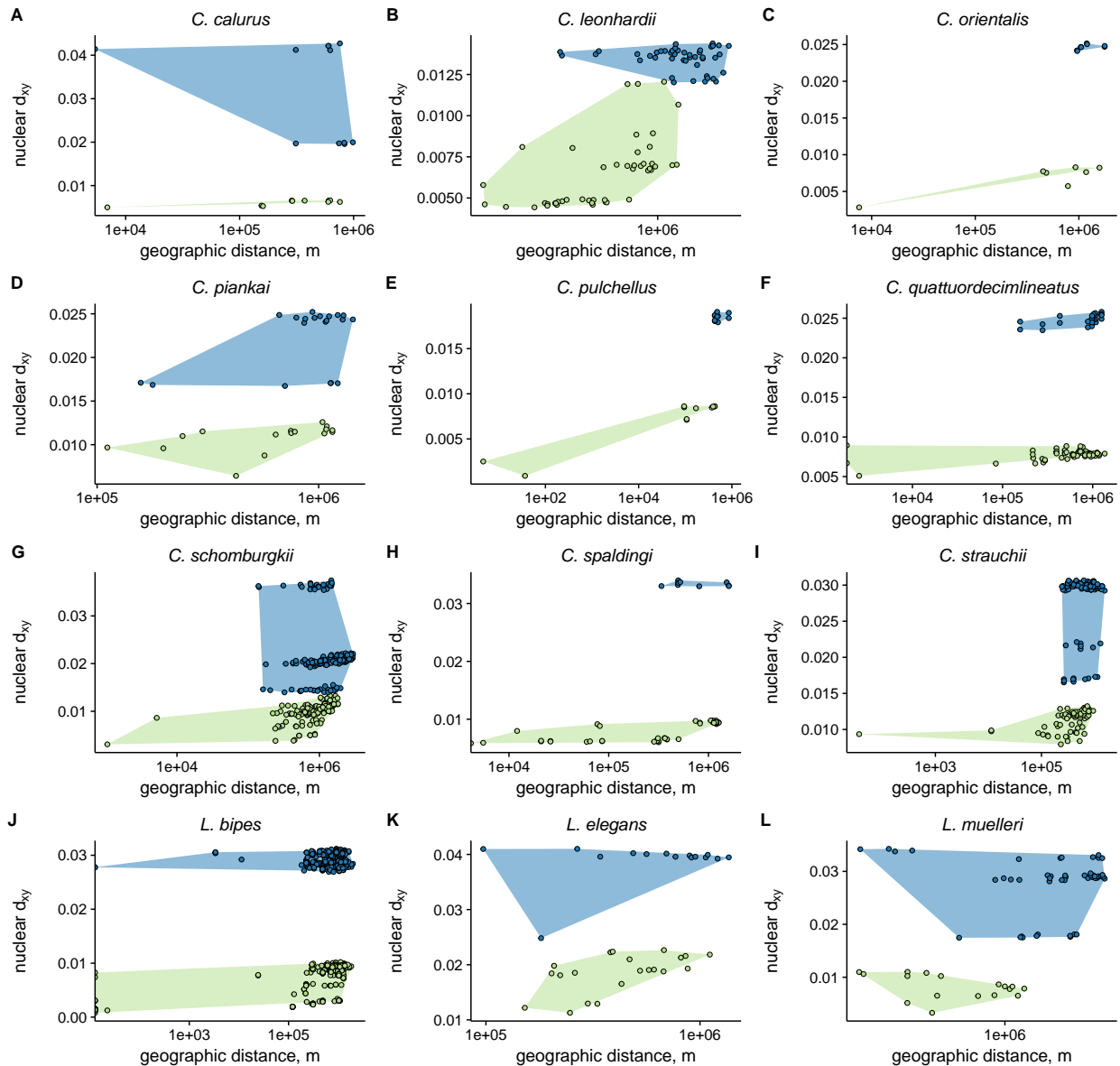


Figure S13: Patterns of pairwise genetic differentiation (d_{xy}) for 12 nominal sphenomorphine species. Putatively new operational taxonomic units (OTUs) were identified in each of these species using a coalescent-based species delimitation approach. Green points are estimates taken between individuals in the same OTU; blue points are taken between individuals in different OTUs. Each graph shows that between-OTU comparisons exhibit significantly great d_{xy} than within-OTU comparisons at the same geographic distance. This pattern suggests that these units are not exchanging genes and that they are evolving independently. If the OTUs were united by gene flow, we would expect that these points would not show such sharp discontinuities across geographic distance. Rather, we would see a continuous isolation-by-distance pattern within- and between-OTUs.